Plastics, Rubber and Composites Processing and Applications **20** (1993) 239–247

Wear of natural rubber and styrene butadiene rubber vulcanizates at elevated temperatures

P. Thavamani & Anil K. Bhowmick
Rubber Technology Centre, Indian Institute of Technology, Kharagpur 721 302, India

(Received 4 March 1992; revised version received 3 November 1992; accepted 15 November 1992)

Abstract: The effect of carbon black loading, testing temperature and ageing on the abrasion loss (V), dynamic coefficient of friction (μ) and frictional force (F) of natural rubber (NR) and styrene-butadiene rubber (SBR) vulcanizates is reported. The value of V increases with temperature in spite of decreasing μ and F. After ageing, V of gum SBR is less than that of unaged samples due to resin formation. The value of V decreases with carbon black loading. The abradability (A) is related to the reciprocal of breaking energy (E_b) by $A = C/E_b$, where C is a constant having value of the order of 10^{-12} m^3. Ridges are observed on the abraded surface of NR and SBR. The ridge spacing decreases with carbon black loading and increases with testing temperature. The abrasion loss increases linearly with ridge spacing.

Introduction

Wear of rubber is an important subject both technically and commercially, since it determines the life of many rubber products, particularly tyres of various kinds. Though considerable research work has been done, the scientific understanding needed to predict the wear of a rubber product under specified conditions is still lacking. This is due to the fact that the mechanism of abrasion depends on many parameters, such as the nature of the polymer and abrader, frictional force, humidity, velocity, temperature and pressure. This is further complicated by thermochemical, mechanochemical and oxidative degradations.

Unlike plastic materials, the abraded surfaces of rubber develop ridges, called abrasion patterns, perpendicular to the direction of abrasion. Schallamach[1] first reported this pattern formation using a needle as an abrader. He explained that the ridges were bent back, exposing the underneath for further abrasion before the tongue was torn off. Bhowmick[2] noted that the patterns on abraded surfaces were formed due to the coalescence of small rubber particles. Champ *et al.*[3] and Thomas[4] studied the abrasion using a razor blade as an abrader. They suggested that the abrasion was caused by cumulative growth of cracks under the action of frictional force and the dependence of the rate of abrasion on frictional force was similar to the dependence of rate of growth of a crack on tearing force. Later, Gent and Pulford,[5] using the same apparatus as that used by Champ *et al.*[3], reported that abrasion was not solely accounted for by crack growth, and that other fracture mechanisms were also involved. They observed the formation of an oily layer on the abraded surface of natural rubber (NR), styrene-butadiene rubber (SBR) and ethylene propylene rubber (EPR) due to extensive thermomechanical degradation. Schallamach,[6] and later Pulford,[7] reviewed the mechanisms of tyre wear. Tread wear is caused predominantly by surface degradation by oxidation and is accelerated by hysteretic heating and fatigue due to dynamic stress. Hence laboratory results obtained at room temperature have little significance in predicting the performance rating of a tyre tread.[8]

We have developed some suitable compounds, based on NR and SBR, for battle tank track pads. During use in the field the track pads were damaged by excessive wear; chipping and subsequent chunking of large pieces of rubber were enhanced by the high temperatures generated. The present study is aimed at understanding the mechanism of wear at elevated temperature, i.e. when the viscoelastic energy dissipation is much reduced. We report here our investigations on the effect of temperature on the abrasion loss (V), dynamic coefficient of friction (μ) and frictional force (F) of NR and SBR at different carbon black loadings. The morphology of the abraded surface was studied using scanning electron microscopy (SEM).

Experimental

Materials used

NR and SBR (Synaprene 1502) were obtained from Dunlop (India) Ltd, Sahaganj, India. Carbon black (N110) was supplied by Philips Carbon Black Ltd, Durgapur, India. Other materials, such as zinc oxide, stearic acid, sulphur, etc., were of chemically pure grade.

Abrasion specimen preparation

All the compounds given in Table 1 were mixed in a laboratory mill as per the standard procedure. The rubber specimens for abrasion (20×20 mm^2) were prepared by moulding in an electrically heated hydraulic press at 160°C to its optimum cure state (as determined by rheometry).

Wear apparatus and measurement of μ, V a

A modified Du Pont abrader as shown in Fig. 1 was used to measure the abrasion loss (V), abradability (A), dynamic coefficient of friction (μ) and frictional force (F). Two rubber specimens were clamped on the lever arm and the end of the lever was attached to a load cell to measure the torque and hence the tangential force acting at the rubber–abrader interface. The abrader (silicone carbide abrasive paper, grain size 325 mesh) was fixed on a disc and load was applied normal to the rubber specimens by a hanging weight on the other end of a rod attached perpendicular to the lever arm. The abrader and the rubber specimens were kept in a chamber maintained at a temperature within ±2°C variation by blowing hot air. The experiments were carried out at 25, 50, 75 and 100°C for 10 min after conditioning the samples for 15 min. The abrasion loss for the sample, aged at 100°C for 24 h in a hot air oven, was

Table 1. Formulations used (phr)

Ingredients	Compound reference							
	H1	H2	H3	H4	H5	H6	H7	H8
NR	100	100	100	100	—	—	—	—
SBR	—	—	—	—	100	100	100	00
Zinc oxide	5	5	5	5	5	5	5	5
Stearic acid	6	6	6	6	6	6	6	6
TMQ[a]	0·5	0·5	0·5	0·5	0·5	0·5	0·5	0·5
Santoflex 13[b]	3	3	3	3	3	3	3	3
Carbon black (N110)	—	30	40	50	—	30	40	50
CBS[c]	0·8	0·8	0·8	0·8	0·8	0·8	0·8	0·8
Sulphur	2	2	2	2	2	2	2	2
PVI[d]	0·5	0·5	0·5	0·5	0·5	0·5	0·5	0·5
Total	117·8	147·8	157·8	167·8	117·8	147·8	157·8	167·8

[a]TMQ, 2,2,4-Trimethyl-1,2-dihydroquinoline.
[b]Santoflex 13, *N*-(1,3-Dimethylbutyl)-*N*-phenyl-*p*-phenylene diamine.
[c]CBS, Cyclohexyl-2-benzothiazole sulphenamide.
[d]PVI, Prevulcanization inhibitor, Monsanto.

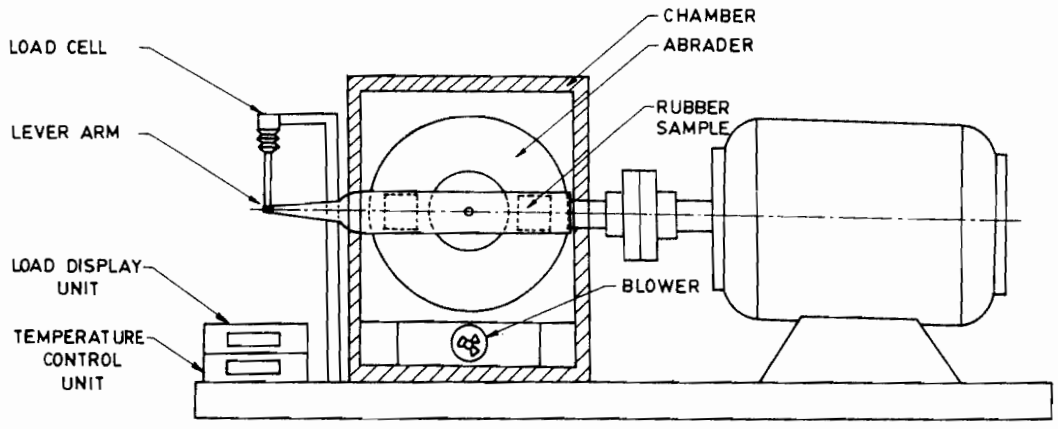

Fig. 1 Schematic diagram of abrader.

also measured. The values for μ, V and A were calculated from the torque and weight loss.

From Fig. 2 the dynamic coefficient of friction μ may be written as[9] (the derivation is given in the Appendix):

$$\mu = 3/2\ \tau/P\left(\frac{R_2^2 - R_1^2}{R_2^3 - R_1^3}\right) \quad (1)$$

where τ = torque (N m) and P = normal load (N).

$$\text{Frictional force } F = \mu P \quad (2)$$

$$\text{Frictional work (per revolution)} \quad W = \frac{\mu \times P \times d}{a}\ (\text{J/m}^2) \quad (3)$$

where d = circumferential length of abrader track (m) and a = area of the specimen in contact with abrader (m^2).

$$\text{Abradability} \quad A = V/W \quad (4)$$

where V = abrasion loss (m^3/rev).

The values reported here are the averages of three separate experiments.

Determination of tensile and tear strength and breaking energy (E_b)

Tensile and tear strength of all the compounds were determined using Zwick UTM 1445 interfaced with a computer. The breaking energy was obtained from the area under the stress–strain curve directly from the interface computer. The results are given in Table 2.

Dynamic mechanical properties

Dynamic mechanical properties, viz. storage shear modulus G' and tanδ were measured using a Polymer Laboratories' PL-DMTA unit in shear mode of deformation with double strain amplitude of 64 μm at 10 Hz and 2°C/min heating rate. The data acquired at 10 Hz were transformed to the fre-

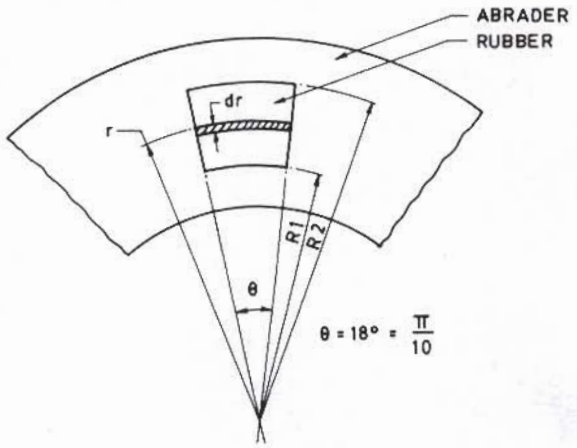

Fig. 2 A segment of rubber–abrader contact surface.

Table 2. Physical properties of compounds

Properties	Compound reference							
	H1	H2	H3	H4	H5	H6	H7	H8
Optimum cure time at 160°C (min)	10	10	10	10	12	12	12	12
Specific gravity	0·95	1·05	1·09	1·13	0·99	1·11	1·14	1·17
Hardness (Shore A)	35	58	63	69	35	56	60	67
Tensile strength (MPa)								
25°C	20	24	27	31	9	17	24	28
100°C	3	7	8	10	2	6	8	10
After ageing at 100°C for 24 h	6	12	13	14	7	10	18	26
300% modulus (MPa)	1·3	6·5	9·1	14·2	1·5	5·3	8·5	12·1
Elongation at break (%)	1100	730	650	480	700	660	620	580
Tear strength (N/cm)								
25°C	370	720	860	930	260	380	520	650
100°C	110	240	350	440	85	130	310	480
Tanδ								
25°C	0·133	0·149	0·158	0·171	0·142	0·152	0·165	0·189
100°C	0·078	0·131	0·151	0·166	0·115	0·143	0·159	0·178

quency of deformation ($1{\cdot}5 \times 10^4$ Hz, calculated from the number of asperities per unit length (56 per mm) and the velocity of abrasion (16 m/min)) involved during abrasion, using the universal Williams–Landel–Ferry (WLF) rate temperature shift factor log a_T.

$$\log a_T = -17{\cdot}44(T - T_g)/(51{\cdot}6 + T - T_g) \quad . \quad (5)$$

where T_g is the glass transition temperature of rubber.

Microscopic study on abraded surface

The abraded surface was sputter-coated with gold and examined under a scanning electron microscope (SEM) (model No. 2, DV Cam Scan, UK). SEM photographs of the ridges were taken at higher magnification (300–500×) to measure the ridge spacings. All the samples were tested within 48 h.

Results and discussion

Abrasion of gum NR and SBR at high temperature

Figure 3 shows the variation of abrasion loss for NR and SBR gum compounds under different conditions. The volume loss increases with testing temperature for all the compounds. After ageing, the volume loss of NR is higher and that of SBR is lower compared to the corresponding unaged samples. These observations could be explained as follows. At high temperature, the internal viscosity is decreased, the viscoelastic energy dissipation is reduced and hence the rubbers attain a lower strength value.[11] The volume loss accordingly increases with rise of testing temperature. However, we expected a greater difference in volume loss when the samples were tested at 25°C and 100°C. At 100°C, formation of oily layers on the abrader track, due to extensive degradation of the rubber under the mechanical shearing action (like cold mastication) is observed. This oily layer must have acted as a lubricant at the interface and thereby protected the abrading surface from further material removal.

In an attempt to prevent this lubrication effect, experiments were carried out using china clay, rock powder and magnesia dusts, but in all cases the abrasion loss in the presence of the dusts was around ten-fold less. It appears that the dusts get embedded into the cavities on the rough abrader making the abrader surface smooth. Hence, the abrasion loss was less in the presence of dust particles. The volume loss of aged samples is higher than that of unaged samples due to thermo-oxidative degradation of NR. But an opposite trend is observed with SBR compound because it has heat resistance and it undergoes resin formation during ageing.[12] Similar results were reported with Ethylene Propylene Diene Rubber (EPDM) and butyl rubber blends.[13]

Effect of carbon black

The variation of abrasion loss with carbon black loading at different temperatures is shown in Fig. 4. The volume loss decreases with carbon black loading and increases with temperature. At any particular carbon black loading and temperature, the abrasion loss of NR is less than that of SBR compounds. The incorporation of carbon black into rubber reinforces the matrix through network for-

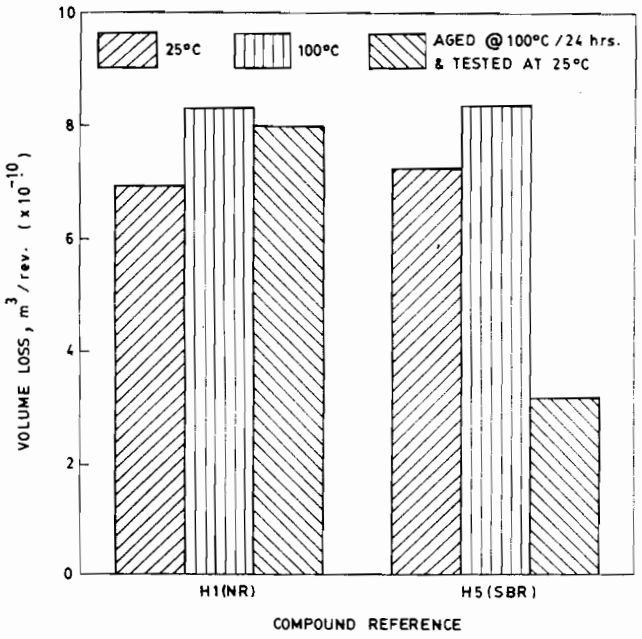

Fig. 3 Variation of abrasion loss with nature of polymer at different conditions.

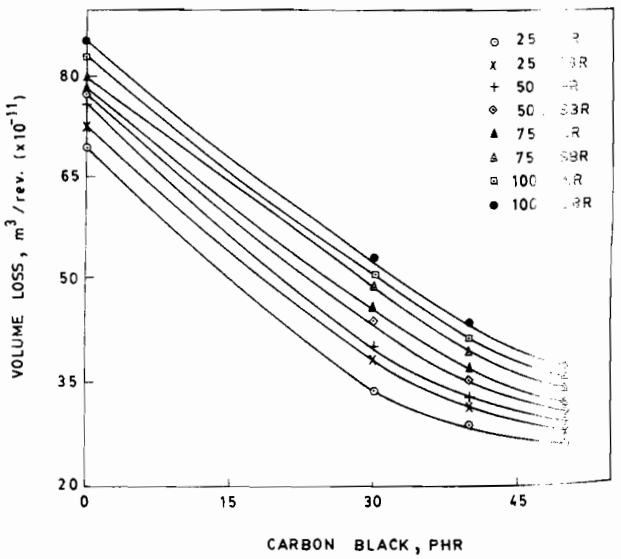

Fig. 4 Variation of abrasion loss with carbon black loading at different temperatures.

mation, hydrodynamic effect and strain amplification[14] and hence abrasion loss decreases with carbon black loading. But when the temperature is increased, the viscoelastic energy dissipation is gradually decreased and this accounts for the increase in volume loss with temperature. Since strain-induced crystallization[15] occurs in NR even at high temperature, the volume loss of NR is less than that of SBR.

Figure 5 shows the variation of μ and F with temperature at different carbon black loadings. The values of μ and F decrease with temperature and increase with carbon black loading. This observation can be explained as follows. The total frictional force (F) generated at the sliding interface consists of two components, adhesional (F_A) and hysteretic (F_H),[16] i.e.

$$F = F_A + F_H \tag{6}$$

F_A is attributed to the molecular bonding between the exposed surface atoms of rubber and abrader. Any sliding action causes these bonds to stretch, rupture and relax before new bonds are formed. The adhesional component, F_A, is predominant when the abrasion is against a smooth surface. The hysteretic component, F_H, arises when the sharp asperities on the rough abrader move over the rubber surface. If F_A and F_H in eqn (6) are replaced by[16]

$$F_A = K_1 S[E'/P^\alpha] \tan\delta \; (\alpha < 1) \tag{7}$$

$$F_H = K_2[P/E']^n \tan\delta \; (n > 1) \tag{8}$$

the total frictional force F becomes

$$F = (K_1 S[E'/P^\alpha] + K_2[P/E']^n) \tan\delta \tag{9}$$

where P is normal load, E' is the storage modulus, S is the effective shear strength of the sliding interface, and α and n are exponents.

Table 2 reports the tanδ values of various compounds. It was reported[17] in our earlier work that tanδ decreased with temperature and increased with carbon black loading. Payne[18] reported that the carbon black network formation significantly increases the E' and E'' at low strain amplitude and E'' is affected to a greater degree and hence tanδ increases with carbon black loading. This explains, in accordance with eqn (9), the increase of μ and F with carbon black loading. Staklis[19] reported similar observation for butyl rubber up to 55–65 phr of Super Abrasion Furnace (SAF) carbon black. With rise of temperature, the hydrodynamic effect and degree of strain amplification are reduced[11] and hence μ and F decrease with temperature. In spite of decreasing frictional force, the volume loss increases with temperature. This may be due to the fact that the critical tearing energy and fatigue resistance are drastically reduced at high temperature.[20] Table 2 shows the strength values at 25°C and 100°C for the compounds studied. There is approximately 60–80% reduction in strength.

Relation between abradability (A) and breaking energy (E_b)

During abrasion against silicone carbide abrader, microcutting, stretching and rupture of particles from the surface take place repeatedly. Grosch and Schallamach[21] reported a linear relation between abradability and reciprocal of breaking energy:

$$A = C/E_b \tag{10}$$

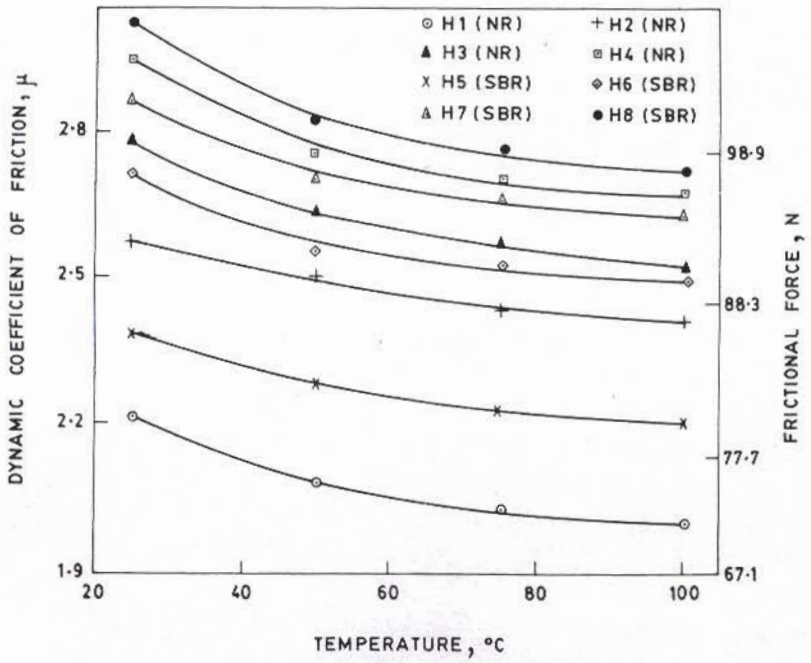

Fig. 5 Variation of μ and F with temperature.

where the coefficient C represents the volume loss per unit frictional work done on a material for which the breaking energy is unity. A similar plot of A versus $1/E_b$ gives a linear relation as shown in Fig. 6. The plot passes through the origin, indicating that there would be no abrasion loss if the breaking energy were infinity. The value of C is in the order of 10^{-12} m^3.

Microscopic studies on the abraded surface

In general, the abraded surface of NR and SBR is tacky, and at 100°C, the formation of a tarry layer and pasty mass on the abrader track is observed (Fig. 7). Close inspection of the abraded surface of NR and SBR under a microscope reveals the presence of ridges perpendicular to the direction of the abrasion. The spacings between adjacent ridges are measured from SEM photographs taken at higher magnification and are reported in Tables 3 and 4. The ridge spacing at any particular temperature decreases with carbon black loading (Figs 8 and 9, Table 3) and increases with temperature (Table 4). At the same carbon black loading and the same testing temperature, the ridge spacing on SBR (Fig. 10) is larger than that of NR. This difference is, however marginal at higher testing temperatures. Schallamach[22] related the ridge spacing (R_s) to Hooke's modulus (E), normal load (P) and diameter of abrasive grain (d') by the following equation:

$$R_s = \text{Const.}(\phi/E)d'(P/E)^{5/9} \quad (11)$$

where $\phi = F/A$; F is the frictional force and A the true area of contact.

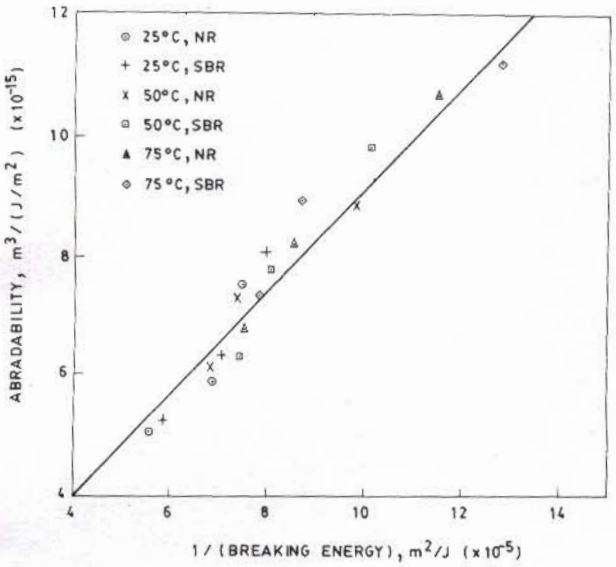

Fig. 6 Relation between abradability and reciprocal of breaking energy.

Table 3. Ridge spacings at 100°C

Compound reference	Ridge spacing[a] (μm)
H1	156 ± 45
H2	93 ± 15
H3	77 ± 15
H4	55 ± 12
H5	165 ± 35
H6	114 ± 17
H7	86 ± 15
H8	67 ± 15

[a]Based on ten measurements on magnified photographs.

Table 4. Ridge spacing at different temperatures[a]

Temperature (°C)	Ridge spacing (μm)	
	H1	H5
25	40 ± 12	53 ± 14
50	64 ± 15	73 ± 15
75	85 ± 15	94 ± 15
100	156 ± 45	165 ± 35

[a]Based on ten measurements on magnified SEM photographs.

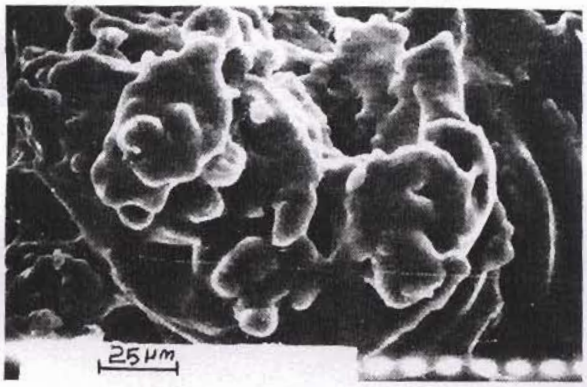

Fig. 7 SEM photograph of tarry residue of abraded debris of compound H2 at 100°C.

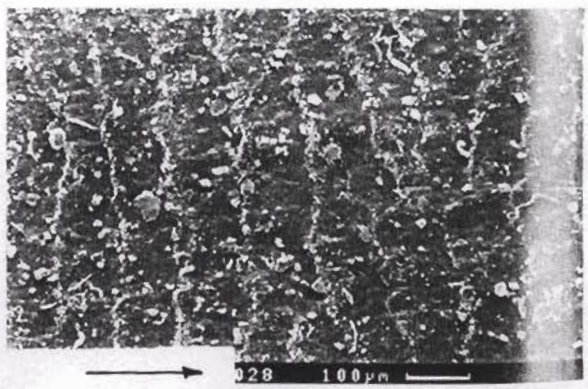

Fig. 8 SEM photograph of abraded surface of compound H1.

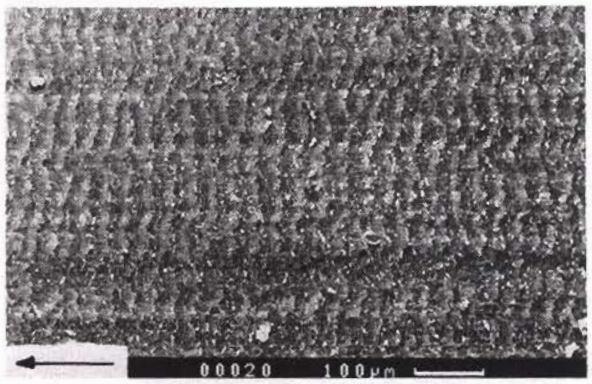

Fig. 9 SEM photograph of abraded surface of compound H4.

Fig. 10 SEM photograph of abraded surface of compound H6.

Since the abrasion is carried out at constant normal load using same abrader, ϕ, P and d' can be considered as constants. Hence eqn (11) could be rewritten as

$$R_s = \text{Const.}\,(1/E)^{1.56} \qquad (12)$$

During abrasion the rubber surface is subjected to shearing and hence E may be replaced by the shear modulus G' and eqn (12) can be written as

$$R_s = \text{Const.}\,(1/G')^{1.56} \qquad (13)$$

In accordance with the above equation, the logarithmic plot of R_s against G' for NR and SBR compounds gives a straight line as shown in Fig. 11.

The abrasion loss is plotted against ridge spacing in Fig. 12. It can be seen that the abrasion loss increases with ridge spacing. The rubber vulcanizates are more susceptible to ridge formation at lower loading of filler and also at higher temperature. Once the ridge is formed, it accelerates the rate of wear[23] and grows with time of abrasion. Hence, abrasion loss increases with ridge spacing which in turn increases with temperature and decreases with carbon black loading.

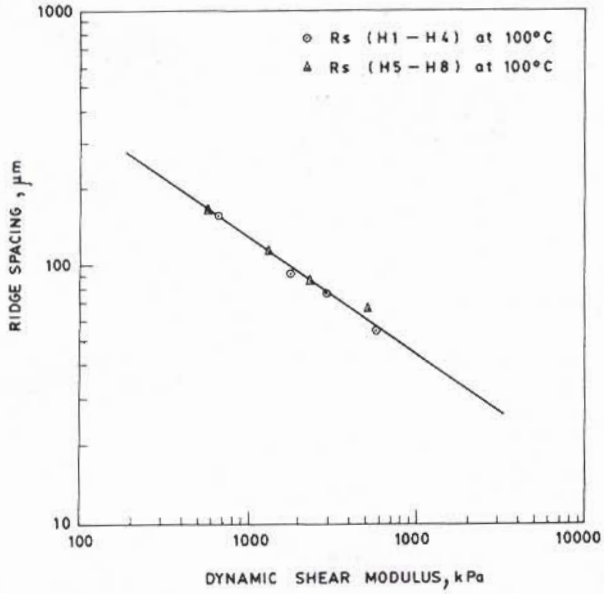

Fig. 11 Relation between ridge spacing, R_s, and dynamic shear modulus, G'.

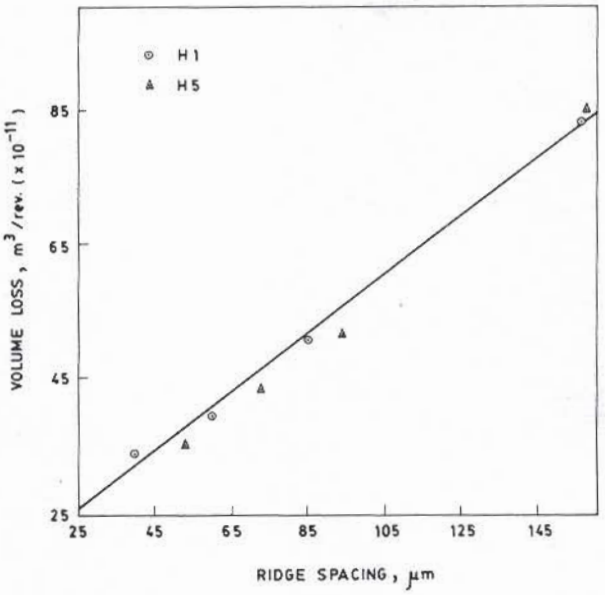

Fig. 12 Relation between abrasion loss and ridge spacing.

Conclusions

(1) The abrasion loss of gum NR and SBR increases with testing temperature. After ageing, the abrasion loss of SBR is less than that of unaged sample due to resin formation, while the NR sample shows a drastic volume loss.

(2) The abrasion loss decreases with carbon black loading even at high temperature.

(3) The abradability increases linearly with reciprocal of breaking energy and the straight line passes through the origin.

(4) Ridges on the abraded surface are observed and the distance between adjacent ridges decreases with carbon black loading and increases with temperature.
(5) The ridge spacing is related to shear modulus G' and the abrasion loss increases linearly with ridge spacing.

References

1. SCHALLAMACH, A., Abrasion and tyre wear. In *Chemistry and Physics of Rubber-Like Substances*, ed. L. Bateman. MacLaren, London, Ch. 13, p. 382.
2. BHOWMICK, A. K., Ridge formation during the abrasion. *Rubber Chem. Technol.*, **55** (1982) 1055.
3. CHAMP, D. H., SOUTHERN, E. & THOMAS, A. G., Fracture mechanics applied to rubber abrasion. *Am. Chem. Soc., Coatings, Plast. Div. Prepr.*, **34** (1) (1974) 237.
4. THOMAS, A. G., Factors influencing the strength of rubbers. *J. Polym. Sci. Symp.*, **48** (1974) 145.
5. GENT, A. N. & PULFORD, C. T. R., Mechanism of rubber abrasion. *J. Appl. Polym. Sci.*, **28** (1983) 943.
6. SCHALLAMACH, A., Recent advances in knowledge of rubber friction and tyre wear. *Rubber Chem. Technol.*, **41** (1968) 209.
7. PULFORD, C. T. R., Failure of rubber by abrasion. *Rubber Chem. Technol.*, **58** (1985) 653.
8. BASSI, A. C., Rubber abrasion test with paper tape. *Rubber Chem. Technol.*, **41** (1968) 1022.
9. THAVAMANI, P. & BHOWMICK, A. K., Wear of tank track pad rubber vulcanizates by various rocks. *Rubber Chem. Technol.*, **65** (1992) 31.
10. FERRY, J. D., *Viscoelastic Properties of Polymers*. Wiley, New York, 1970, p. 274.
11. GENT, A. N., Strength of elastomers. In *Science and Technology of Rubber*, ed. F. R. Eirich. Academic Press, New York, 1978, Ch. 10, p. 427.
12. GRASSIE, N. (ed.), *Developments in Polymer Degradation*, Vol. 1. Applied Science Publishers, London, 1977, p. 171.
13. BHAUMIK, T. K., GUPTA, B. R. & BHOWMICK, A. K., Abrasion of high temperature conveyor belt compounds based on ethylene propylene diene and bromobutyl rubber blends. *Wear*, **128** (1988) 167.
14. DONNET, J. B. & VOET, A. (eds), *Carbon Black — Physics, Chemistry and Elastomer Reinforcement*. Marcel Dekker, New York, 1976, Ch. 8, p. 272.
15. ANDREWS, E. H., Crystalline morphology in thin films of natural rubber. Part 2. Crystallization under strain. *Proc. Roy. Soc. Lond. A*, **277** (1964) 562.
16. MOORE, D. F. (ed.), *The Friction of Pneumatic Tyres*. Elsevier Scientific Publishing, New York, 1975, Ch. 1, p. 4.
17. THAVAMANI, P. & BHOWMICK, A. K., Dynamic mechanical properties of hydrogenated nitrile rubber: effect of cross-link density, curing system, filler and resin. *J. Mater. Sci.*, **27** (1992) 3243.
18. PAYNE, A. R. & WHITTAKER, R. E., Low strain dynamic properties of filled rubbers. *Rubber Chem. Technol.*, **44** (1971) 440.
19. STAKLIS, A. A., Elastomer abrasion at high velocity. *Rubber Chem. Technol.*, **45** (1972) 1241.
20. BHOWMICK, A. K., NEOGI, C. & BASU, S. P., Threshold tear strength of carbon black filled rubber vulcanizates. *J. Appl. Polym. Sci.*, **39** (1990) 917.
21. GROSCH, K. A. & SCHALLAMACH, A., Relation between abrasion and strength of rubber. *Trans. Inst. Rubber Ind.*, **41** (1965) 80.
22. SCHALLAMACH, A., Friction and abrasion of rubber. *Wear*, **1** (5) (1958) 384.
23. SCHALLAMACH, A., Abrasion, fatigue and smearing of rubber. *J. Appl. Polym. Sci.*, **12** (1968) 281.

Appendix: Determination of dynamic coefficient of friction

From Fig. 2, the area of contact of specimen with abrader

$$= \frac{\pi}{20}(R_2^2 - R_1^2) \tag{A1}$$

Let us consider an infinite small element having width dr and radius r. The normal load (P) acting on this element is given by:

$$dp = \frac{P}{\pi/20(R_2^2 - R_1^2)} \times r\,d\theta\,dr \tag{A2}$$

The frictional force acting on this element in dynamic conditions is

$$df1 = dp \times \mu \tag{A3}$$

$$= \mu \times \frac{P \times r\,d\theta\,dr}{\pi/20(R_2^2 - R_1^2)} \tag{A4}$$

Since $df1$ opposes the relative motion between the rubbing surfaces, this force must act tangential to a circle of radius r. At 180° from this, an opposite and an equal reaction force $df2$ is generated. These forces, $df1$ and $df2$, form a couple. Since the entire area can be broken like this, we can conclude that there are only couples in the plane of contact.

So the torque due to all the couples in this infinite small element is given as

$$d\tau = \int_0^{\pi/10} df1 \times r$$

$$d\tau = \frac{\mu \times P}{\pi/20(R_2^2 - R_1^2)} \int_0^{\pi/10} r^2 d\theta\,dr$$

$$d\tau = \frac{\mu \times P}{\pi/20(R_2^2 - R_1^2)} \times r^2\,dr \left[\frac{\pi}{10} - 0\right]$$

Integrating with respect to θ, keeping r constant we get

$$d\tau = \frac{2\mu \times P}{(R_2^2 - R_1^2)} r^2\,dr \tag{A5}$$

Now the torque due to the entire area of contact is obtained by integrating eqn (A5) with respect to r from R_1 to R_2.

$$\int d\tau = \frac{2\mu \times P}{(R_2^2 - R_1^2)} \int_{R_1}^{R_2} r^2 \, dr$$

$$\tau = \frac{2\mu \times P}{(R_2^2 - R_1^2)} \left[\frac{R_2^3 - R_1^3}{3} \right]$$

$$\tau = \frac{2\mu \times P}{3} \left[\frac{R_2^3 - R_1^3}{R_2^2 - R_1^2} \right] \qquad \text{(A6)}$$

This torque can be measured from the force displaced in the load cell display unit.

Hence the dynamic coefficient of friction

$$\mu = \frac{3}{2} \frac{\tau}{P} \left[\frac{R_2^2 - R_1^2}{R_2^3 - R_1^3} \right]$$